PAPER

# Design of an innovative platform for the treatment of cerebral tumors by means of erythro-magneto-HA-virosomes

Biomedical Physics & Engineering Express

PAPER

# Design of an innovative platform for the treatment of cerebral tumors by means of erythro-magneto-HA-virosomes

**Gioia Lucarini**[1,2], **Francesca Sbaraglia**[1,2], **Alessio Vizzoca**[3], **Caterina Cinti**[3], **Leonardo Ricotti**[1,2] and **Arianna Menciassi**[1,2]

[1] The BioRobotics Institute, Scuola Superiore Sant'Anna, Piazza Martiri della Libertà 33, 56127 Pisa, Italy
[2] Department of Excellence in Robotics & AI, Scuola Superiore Sant'Anna, Piazza Martiri della Libertà 33, 56127 Pisa, Italy
[3] Institute of Organic Synthesis and Photoreactivity (ISOF)- Department of Chemical Sciences and Materials Technologies (DSCTM), National Research Council of Italy (CNR), via Piero Gobetti 101, 40129, Bologna, Italy

**E-mail:** g.lucarini@santannapisa.it

**RECEIVED**
11 January 2020

**REVISED**
2 April 2020

**ACCEPTED FOR PUBLICATION**
16 April 2020

**PUBLISHED**
7 May 2020

**Keywords:** cell-based drug delivery system, magnetic localization, magnetic platform, erythro-magneto-HA-virosome, magnetic medical devices

## Abstract

Gliomas are the most common intracranial tumors, featured by a high mortality rate. They represent about 28% of all primary central nervous system (CNS) tumors and 80% of all malignant brain tumors. Cytotoxic chemotherapy is one of the conventional treatments used for the treatment, but it often shows rather limited efficacy and severe side effects on healthy organs, due to the low selectivity of the therapy for malignant cells and to a limited access of the drug to the tumor site, caused by the presence of the Blood-Brain Barrier. In order to resolve these limitations, recently an Erythro-Magneto-HA-Virosome (EMHV) drug delivery system (DDS), remotely controllable through an externally applied magnetic field, has been proposed. To accurately localize the EMHV at the target area, a system able to generate an adequate magnetic field is necessary. In this framework, the objective of this paper was to design and develop a magnetic helmet for the localization of the proposed EMHV DDS in the brain area. The results demonstrated, through the implementation of therapeutic efficacy maps, that the magnetic helmet designed in the study is a potential promising magnetic generation system useful for studying the possible usability of the magnetic helmet in the treatment of glioma and possibly other CNS pathologies by EMHV DDS.

## 1. Introduction

Sample Gliomas are the most common intracranial tumors, arising from glial cells and mainly affecting the brain. They are fastly growing and infiltrating tumors, featured by a high mortality rate. They represent about 28% of all primary central nervous system tumors and 80% of all malignant brain tumors (Ostrom *et al* (2013)).

Cytotoxic chemotherapy is one of the conventional treatments used to face gliomas. It often shows rather limited efficacy and severe side effects on healthy organs, due to the low selectivity of the therapy for malignant cells and to a limited access of the drug to the tumor site, caused by the presence of the Blood-Brain Barrier (BBB). The BBB hinders, in fact, the passage of nearly 98% of therapeutic molecules administered systemically (Abbott 2013).

Several research efforts currently focus on site-specific controlled drug delivery systems (DDS), to increase therapy effectiveness and reduce the mentioned side effects (Ricotti *et al* (2015)). Nanoscale DDS, such as liposomes, micelles or polymer-based nanoparticles, have been designed to improve the solubility and circulation time of drugs administered parenterally (Moghimi *et al* (2001), Wilhelm *et al* 2016). However, nanocarriers show a low drug loading capability, due to their small size (typically few tens of nanometers).

To improve the capability of carrying large amounts of drugs, cell-based DDS have been proposed (Pierige *et al* (2008)). In addition to the mentioned higher drug loading capability, such carriers show other advantages in comparison with nanosized ones, such as prolonged circulation times and intrinsic biocompatibility, thanks to cell membrane epitopes on

the external DDS shell, recognized as 'self' components by the organism. In particular, erythrocytes appear a promising option as DDS to be used in humans (Rossi *et al* (2005), Muzykantov 2010).

On the other hand, cell-based DDS raise the need to elaborate strategies to effectively and safely control their therapeutic action. In fact, being featured by a micrometric size, they cannot rely on the enhanced permeation and retention (EPR) effect to accumulate at the tumor site, differently from their nano-sized counterparts (Greish 2010). This means that cell-based DDS must be provided with a mechanism that enables their remote control, in order to guarantee a targeted and effective therapy. Among the different strategies that can be used to provide DDS with a good degree of controllability (Timko *et al* 2010, Mura *et al* (2013)), the use of magnetic fields seems to be one of the most promising and clinically usable solutions (Tabatabaei *et al* (2015), Price *et al* (2018), Liu *et al* (2019)).

In this framework, an interesting erythrocyte-based DDS, remotely controllable through an externally applied magnetic field, has been recently proposed (Cinti *et al* (2011), Grifantini *et al* (2018)). This vector, named erythro-magneto-HA-virosome (EMHV), consists of an engineered erythrocyte provided with hemagglutinin (a viral spike fusion glycoprotein) on its membrane and embedding superparamagnetic nanoparticles and an anti-cancer drug. The action mechanism of this system is grounded on the ability of hemagglutinin to fuse with the target cell membrane, thus releasing in it the therapeutic compound. This process occurs when the EMHV DDS is magnetically attracted to the target cell and forced to keep its position for a few minutes against the blood flux. Once this happens, the hemagglutinin triggers the fusion of the EMHV membrane with the capillary cell wall. Then, the therapeutic compound embedded in the EMHV is released in the extravascular compartment (thus, if the EMHV is properly targeted, the drug reaches the tumor cells). This targeting strategy allows to increase the therapy selectivity and to minimize the off-side toxicity (Cinti *et al* (2011)).

To effectively localize EMHVs at the target area, a system able to generate an adequate magnetic field is necessary. To date, no permanent magnets-based actuation systems have been designed specifically for the anchoring of EMHVs. Indeed, so far, EMHVs have been tested simply by approaching a small permanent magnet on the animal model skin surface, without any theoretical effort aimed at optimizing it (Lande *et al* (2012), Naldi *et al* (2014), Grifantini *et al* (2018)). While this approach can be somehow effective in rodents, in which deep body regions are relatively close to the outer skin surface, when dealing with deep human body tissues (e.g., to target gliomas in the brain), a more elaborated design effort is needed. This paper reports the design of a helmet able to generate a non-uniform magnetic field in order to localize EMHVs at different possible brain tumor sites, thus enabling the release of drugs in the target area by EMHVs.

The paper is organized as follows: section 2 describes the theoretical background for an EMHV moving in a vessel under the effect of magnetophoretic and drag forces. Section 3 illustrates the steps followed to design the magnetic helmet. The analytical model used to compute the target value of the magnetic field required to anchor the EMHVs at the target site and the requirements and constraints for the magnetic helmet design are described. Magnetic characterization of the EMHVs and the consequent optimal design of the magnetic helmet are also reported in this section. The magnetic field map generated by the magnetic helmet and therapeutic efficacy maps, for studying the possible usability of the magnetic helmet and EMHV DDS in the treatment of glioma, are reported in section 4. The discussion and conclusion are illustrated in section 5.

## 2. Theoretical background

An EMHV in the bloodstream, within a vessel and subjected to an external non uniform magnetic field, experiences several forces. The predominant ones are the viscous drag forces, the magnetophoretic forces due to the field source, buoyancy and gravity. By assuming the EMHV moving in an arteriole (i.e. in the microcirculation area, with typical diameter ranging between 10 $\mu$m and 100 $\mu$m and with a Reynolds number $R_e \ll 1$), a fully developed laminar flow can be considered and all the inertial forces, which are several orders of magnitude smaller than viscous ones, can be neglected (Haverkort *et al* (2009)). Based on this consideration, in this paper only magnetophoretic $\vec{F}_m$ and drag forces $\vec{F}_f$ were taken into account. Moreover the EMHVs suspension is assumed to be diluted in the blood and the erythrocyte volume concentration to be small, therefore the total volume occupied by the EMHVs per unit of fluid volume (defined as c) is considered much less than 1. In this case, also EMHV-blood interactions can be neglected (Furlani and Ng (2006)).

When the EMHV is far enough from the magnetic field source and the effect of the magnetic field on it is negligible, the carrier moves with a velocity $\vec{v}_{EMHV}$ coincident with the blood flow velocity $\vec{v}_f$. Once approaching the area where the magnetic field is stronger, the EMHV experiences a magnetophoretic force $\vec{F}_m$ that deflects its trajectory toward the magnetic field source. As shown in figure 1, the EMHV is decelerated and the velocity change generates a drag force $\vec{F}_f$ in the opposite direction respect to $\vec{F}_m$. In order to anchor the EMHVs at the tumor site, the following condition has to be satisfied:

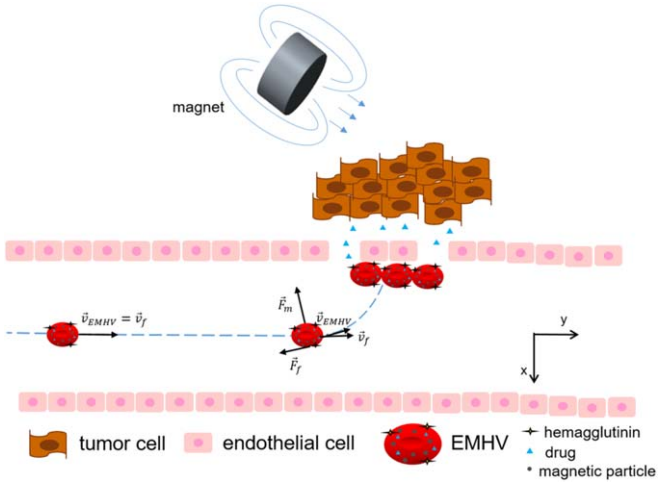


**Figure 1.** Trajectory of an EMHV and forces acting on it while moving in a blood vessel under the effect of an external magnetic field.

$$\vec{F}_m + \vec{F}_f > 0 \tag{1}$$

The magnetophoretic force $\vec{F}_m$ is generated by the difference in the magnetic permeability of the EMHV and the one of the medium surrounding it, in addition to the external magnetic field. This causes the EMHV motion towards regions in which the magnetic field is stronger (Jones 1995).

$$\vec{\mathrm{F}}_m = \mu_f(\mathrm{m}_{eff} \cdot \vec{\nabla})\vec{H} \tag{2}$$

where the EMHV is modeled as a sphere with radius $R_{EMHV}$ and magnetization $\vec{\mathrm{M}}_{EMHV}$ and is replaced by an equivalent point dipole with a moment $\vec{\mathrm{m}}_{eff}$.

The effective dipole moment of such a sphere is calculated as:

$$\vec{\mathrm{m}}_{eff} = 4\pi {R_{EMHV}}^3 \left[ \frac{\mu_0 - \mu_f}{\mu_0 + 2\mu_f}\vec{H} + \frac{\mu_0}{\mu_0 + 2\mu_f}\vec{\mathrm{M}}_{EMHV} \right] \tag{3}$$

The parameters $\mu_f$, $\mu_{0,}$ $R_{\mathrm{EMHV}}$ and $\vec{H}$ are respectively the blood permeability, the permeability of free space ($4\pi 10^{-7}\frac{H}{m}$), the radius of EMHV and the external applied magnetic field. If the EMHV with susceptibility $\varkappa_{EMHV}$ is below saturation, the magnetization is:

$$\vec{M}_{EMHV} = \varkappa_{EMHV}\vec{H_{in}} \tag{4}$$

where $\vec{H_{in}}$ is the internal magnetic field that can be expressed as a function of the external applied magnetic field $\vec{H}$ and the self demagnetization field $\vec{H_{demag}}$ that opposes $\vec{H}$, $\vec{H_{in}} = \vec{H} - \vec{H_{demag}}$.

When EMHVs are magnetized below their saturation level, the effective moment is simplified to:

$$\vec{\mathrm{m}}_{eff} = V_{EMHV}\frac{3(\varkappa_{EMHV} - \varkappa_f)}{[(\varkappa_{EMHV} - \varkappa_f) + 3(\varkappa_f + 1)]}\vec{H} \tag{5}$$

where $\varkappa_f$ is the magnetic susceptibility of the blood and $V_{EMHV}$ is the carrier volume. Substituting equation (5) into equation (2) and considering $|\varkappa_f| \ll 1$ (i.e. $\mu_f \approx \mu_0$) we have:

$$\vec{\mathrm{F}}_m = \mu_0 V_{EMHV}\frac{3(\varkappa_{EMHV} - \varkappa_f)}{[(\varkappa_{EMHV} - \varkappa_f) + 3]}(\vec{H} \cdot \vec{\nabla})\vec{H} \tag{6}$$

The drag force $\vec{F}_f$ is the force acting in the opposite direction respect to the relative motion between the EMHV and the blood. Assuming the EMHV a sphere moving in a laminar flow regime with velocity $\vec{v}_{EMHV}$, the drag force is given by Stoke's law as (Batchelor 1970):

$$\vec{F}_f = -6\pi\eta_f R_{EMHV}(\vec{v}_{EMHV} - \vec{v}_f) \tag{7}$$

where $\eta_f$ is the blood viscosity and $\vec{v}_f$ is the blood velocity.

## 3. Design of the magnetic helmet for HMHVs anchoring

### 3.1. Approach and analytical model

A glioma placed in the hypothalamus, at the center of the brain, was chosen as a possible case study. A human head has an average circumference of 57 cm (Bushby *et al* (1992)). It also has a vertical distance, measured from the nasal root depression between the eyes to the top of the head, equal to 11.2 cm and a vertical distance, measured from the tip of the chin to the top of the head, equal to 23.2 cm (Poston 2000). These anatomical distances were taken into account for designing a magnetic helmet able to exert a magnetophoretic force to stop EMHVs on the vessel walls, thus enabling the hemagglutinin-mediated membrane fusion and drug release at the target.

First, the value of the magnetic field $B_{target}$ necessary to capture the EMHV in the human vasculature and to anchor it at the tumor site was estimated using an analytical model based on the one proposed by Furlani and introduced in the section above (Furlani and Ng (2006)). The trajectory of an EMHV with radius

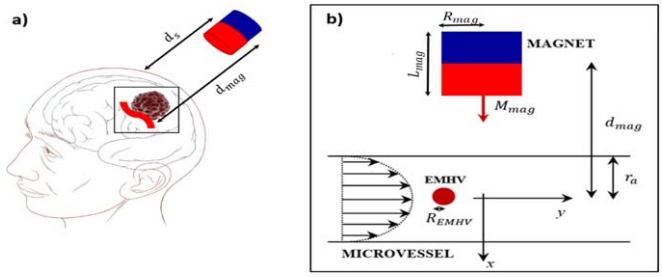


**Figure 2.** (a) Sketch of the head and external NdFeB magnet: the magnet is placed at a distance of dmag from the reference frame with the origin in the tumor site and a distance of ds from the skull, (b) Geometry and reference frame used for the analysis in the analytical model.

$R_{EMHV}$ flowing through a tumor vessel of radius $r_a$ was studied, in proximity to a magnetic field generated by a source positioned outside the body, at distance $d_{mag}$ from the vessel (figure 2(a)) (Furlani and Ng (2006)).

Permanent magnets and electromagnets were compared, as possible solutions to generate the magnetic field needed. Permanent magnets are convenient because they require smaller dimensions, with respect to electromagnets, to generate the desired magnetic field at a certain distance.

Considering that, NdFeB N52 magnets were selected because they are the strongest type of permanent magnets currently available.

We considered a magnet with radius $R_{mag}$, assumed with an infinite length, with its axis orthogonal to the blood flow and featured by a magnetization $M_{mag}$ (figure 2(b)). The dipole model for approaching the problem and deriving $M_{mag}$ is justified because the working distances are much larger than $R_{mag}$ (see section 3.4). Thus, this model can be used to study the effect of the generated magnetic field on the EMHV. A capture condition for EMHVs was established as follows (Furlani and Ng (2006)):

$$\frac{\mu_o \pi {R_{EMHV}}^2 3\left[\frac{\varkappa_{EMHV}}{\varkappa_{EMHV}+3}\right]{M_{mag}}^2}{32\eta_f \bar{v}_f r_a (1+\alpha)^4} > 1 \qquad (8)$$

where $\bar{v}_f$ is the average blood velocity and $\eta_f$ is the blood viscosity. The coefficient $\alpha$ is an adimensional parameter defined as follows: $\alpha = \frac{d_{mag}}{R_{mag}} - 1$.

Starting from the capture condition expressed in equation (8), it is possible to calculate the minimum value of the magnetization $M_{mag\_min}$ of a single external permanent magnet needed in order to stop the EMHVs:

$$M_{mag\_min} = \sqrt{\frac{32\eta_f \bar{v}_f r_a (1+\alpha)^4}{\mu_o \pi {R_{EMHV}}^2 3\left[\frac{\varkappa_{EMHV}}{\varkappa_{EMHV}+3}\right]}} \qquad (9)$$

Considering equation (9), it is possible to calculate the components (i.e., $B_{target\_x}$ and $B_{target\_y}$) of the magnetic field needed for the capture, as follows:

$$B_{target\_x} = \mu_0 \frac{M_{mag\_min}{R_{mag}}^2}{2} \frac{((x+d_{mag})^2 - y^2)}{((x+d_{mag})^2 + y^2)^2} \qquad (10)$$

$$B_{target\_y} = \mu_0 \frac{M_{mag\_min}{R_{mag}}^2}{2} \frac{2((x+d_{mag})y)}{((x+d_{mag})^2 + y^2)^2} \qquad (11)$$

As reported by equations (10) and (11), the required magnetic field depends on the position of the EMHV. In the center of the vessel and perpendicularly to the position of the external magnet (i.e., $x = d_{mag}$ and $y = 0$), the magnetic field assumes the maximum values (figure 2(a)). Considering that the target value of the magnetic field module is:

$$|B_{target}| = \sqrt{(B_{target\_x}(d_{mag}, 0))^2 + (B_{target\_y}(d_{mag}, 0))^2} \qquad (12)$$

This value has to be reached by the superposition principle by considering the sum of the magnetic fields produced by several magnets in the helmet.

### 3.2. Magnetic characterization of the EMHVs

In order to effectively predict the EMHV behavior under the effect of an external magnetic field, a magnetic characterization of the EMHVs was performed, to assess the actual volume magnetic susceptibility $\varkappa_{EMHV}$ (Grifantini *et al* (2018)). The magnetization curves were obtained for different EMHVs samples, using a vibrating sample magnetometer (PPMS 6000, Quantum Design Ltd). The EMHVs samples consisted of human red blood cells with embedded superparamagnetic nanoparticles (Nanocs Inc., Boston USA) and 5-Aza-2-deoxycytidine (Sigma-Aldrich, St Louis, MO, USA) as a drug model. The EMHVs were obtained through a protocol reported in (Cinti *et al* (2011)). Magnetization curves allowed to estimate the specific magnetization M in emu/g at a particular magnetic field strength H (in Oe). This is related to the magnetic susceptibility through the following equation:

$$\varkappa_{EMHV} = \frac{M}{H}\rho_{EMHV} \qquad (13)$$

where $\rho_{EMHV} = 1100\ \frac{\mathrm{Kg}}{\mathrm{m}^3}$ is the average EMHV sample density. The magnetic susceptibility of EMHV is $1.4102 \cdot 10^{-5} \pm 0.1213 \cdot 10^{-5}$.

### 3.3. Requirements and constraints for the magnetic helmet design

In order to generate the magnetic field necessary to anchor the EMHVs at the tumor site, a hemispherical support with radius $R_s$, hosting different magnetic field sources, was designed, taking into account the typical human head size and the need to minimize the helmet's dimensions. Multiple magnetic field sources were preferred respect to a single bigger one, in order to limit the helmet's dimensions and to exploit multiple effects of single magnets (i.e., superposition effect). There was the need to place the magnetic field sources as close as possible to the patient's head, because the magnetic field decays according to $1/r^3$ at relatively large distances. This, together with the anatomical constraints, led to set a support radius $R_s = 12$ cm. The magnetic field generated by the helmet should be equal to $|B_{target}|$ at the center of the brain and should be smaller than $B_{target}$ at superficial brain regions, in order to anchor EMHVs only at the tumor site, which is supposed to be in the brain center. Starting from these requirements, the solution proposed consisted of NdFeB N52 magnets organized in order to generate a magnetic field smaller than $|B_{target}|$ at small distances from the magnets, i.e., close to the skull surface. This solution should avoid the anchoring of EMHVs in undesired regions, thus minimizing off-target drug release and consequent side effects. This choice concerned NdFeB magnets that, positioned on the mentioned hemispherical support, thus placed at a distance $d_{mag} = 12$ cm from the tumor site (figure 2(b)), produce a magnetic field $B_s$, evaluated along the magnet axis at distance $d_s = 2$ cm from the magnet (i.e., at the brain surface), which satisfies the following condition:

$$|B_s| = |B(\bar{x}, 0, 0)| < |B_{target}| \tag{14}$$

where $\bar{x} = -(d_{mag} - d_s)$.

If the magnets arranged on the hemispherical support are far enough from each other (i.e., distance bigger than the radius of the magnets), the magnetic field $B_s$, generated by each magnet at a distance $d_s$ from it, is not affected by the magnetic field produced by all the other magnets. In other words, we can suppose that when the distance between the magnet and the skull is small ($\leqslant R_{mag}$) only the single magnet is responsible for the magnetic field generated in the specific portion of the head. On the other hand, when the target area is deep in the brain, all external magnets contribute to the generation of the magnetic field, thus making possible the generation of a total field adequate for stopping carries (i.e., in terms of magnetic field, what is lost with the distance can be compensated by the larger number of magnets). Thus, it is possible, with the described strategy, to satisfy the condition (14), limiting the magnetic field at the surface of the brain and keeping it below the $B_{target}$ value.

### 3.4. Computation of the magnetic field $B_{target}$ for anchoring the EMHVs

We considered the case of EMHVs moving in an arteriole with radius $r_a = 25\ \mu$m (Vennemann *et al* 2007). The choice to consider an arteriole is an approximation and it represents the worst case because here, the contribution of the fluidic forces is bigger than in a capillary's one. The blood was approximated to be a Newtonian and incompressible fluid having viscosity $\eta_f = 0.001$ Pa · s, density $\rho_f = 1000\ \frac{\text{kg}}{\text{m}^3}$ (Rotariu and Strachan (2005)) and volume magnetic susceptibility $\varkappa_f = -6.6 \cdot 10^{-7}$ (Lunnoo and Puangmali (2015)). The blood flow was considered laminar. Measurements of blood flow exhibited differences in blood velocity between the tumoral and the normal microvasculature. In this study the average blood velocity was assumed in the range $0.1\ \frac{\text{mm}}{\text{s}} \leqslant \bar{v}_f \leqslant 1\frac{\text{mm}}{\text{s}}$ in tumoral arterioles and $1\ \frac{\text{mm}}{\text{s}} \leqslant \bar{v}_f \leqslant 10\ \frac{\text{mm}}{\text{s}}$ in normal arterioles (Rotariu and Strachan (2005)). The magnetic helmet was designed to generate a magnetic field capable of stopping EMHVs moving through an arteriolar blood flow with a maximum velocity $\bar{v}_f = 1\ \frac{\text{mm}}{\text{s}}$. Decreasing the blood flow velocity, the magnetic field required to anchor the EMHVs at the tumor site decreases. Considering the EMHV as a spherical particle with radius $R_{EMHV} = 4\mu$m and magnetic susceptibility $\varkappa_{\text{EMHV}} = 1.4102{*}10^{-5}$, the analytical model proposed in section 3.1 was used to compute the target value $B_{target}$. As shown in figure 2(b), a magnet having infinite extension and radius $R_{mag} = 3$ cm, was located at distance $d_{mag} = 15$ cm from the tumor vessel, where $d_{mag}$ is the distance between the center of the magnet and the center of the vessel. Such value for $d_{mag}$ was chosen according to the value $R_{mag}$, to compute $B_{target}$ at distance $d = 12$ cm from the magnet surface, which corresponds to the case of study. The minimum value for magnetization $\text{M}_{mag\_min} = 2.36{*}10^7\ \frac{A}{m}$ required for EMHV capture was estimated using equation (9). Equations (10)–(12) were used to compute the magnetic field $B$ generated from the magnet along the axis of the arteriole ($-4\ R_{mag} \leqslant y \leqslant 4\ R_{mag}$). The plot of the absolute value of the magnetic field $|B|$ estimated by the analytical model is shown in figure 3(a).

Notice that $|B|$ reaches its maximum value ($|B|_{\text{max}} = 0.6\ T$) at the center of the magnet (y = 0). Such value was considered as the target value $B_{target}$ for anchoring EMHV. It is worth mentioning that any other value for $R_{mag}$ can be used to compute the magnetic field $B_{target}$ by the analytical model. The value of $d_{mag}$ varies according to the value $\text{R}_{mag}$ in order to estimate the magnetic field at a distance $d = 12$ cm from the magnet surface, but the value for $B_{target}$ remains the same if the same magnetic properties of the EMHVs ($\varkappa_{EMHV}$) and the same fluid dynamic ($\bar{v}_f$) and geometric conditions ($r_a$, $R_{EMHV}$) are considered.

Magnetic and fluid dynamic simulations with the commercial FEM code COMSOL Multiphysics 5.2a were performed in order to verify the results obtained by the analytical model and to predict the EMHVs behavior under the effect of the magnetic field computed by the analytical model. Denoting with $\eta$ the capture efficiency, i.e., the fraction of EMHVs

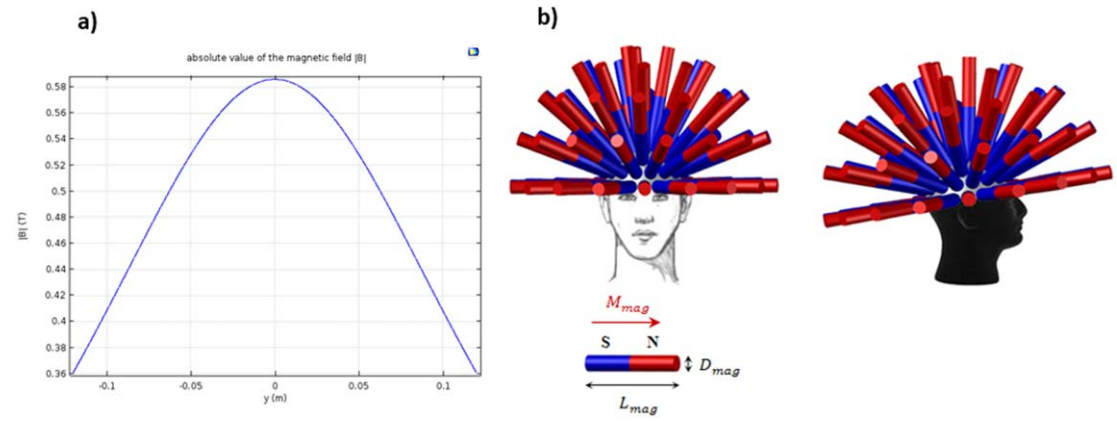


**Figure 3.** (a) Absolute value of the magnetic field |B| (T) evaluated along the axis of the arteriole y between y = −4 $R_{mag}$ and y = 4 $R_{mag}$, (b) Optimal configuration of the NdFeB magnets placed on the hemispherical support. Each magnet has magnetization $M_{mag}$ = 1.1*[10] ^6 A $m^{-1}$ along the main axis, radius $D_{mag}$ = 4 cm and length $L_{mag}$ = 30 cm.

captured by the external magnetic field at the target site, it was observed that a capture efficiency $\eta = 88\%$ was obtained by the magnetic field computed by the analytical model along the tumor arteriole.

### 3.5. Optimal configuration of the magnetic helmet

Considering $|B_{target}| = 0.6\ T$ as the target value needed to anchor EMHV at the target site and considering the radius ($R_s$ = 12 cm) of the hemispherical support in which NdFeB magnets are placed, several configurations of NdFeB N52 magnets were tested, in order to obtain the $B_{target}$ value at the tumor site. A parametric study using COMSOL Multiphysics 5.2a simulations combined with MATLAB scripts (Mathworks, Inc., Natick, MA) was carried out by varying dimensions, magnetization and positioning of the NdFeB magnets on the hemispherical support, to compute the optimal configuration of the NdFeB magnets and obtain the highest magnetic field value at the target site. In particular, the optimization equations of the parametric study (i.e., in terms of $R_{mag}$, $L_{mag}$, $M_{mag}$) which were considered are the following:

$$\begin{cases} \sum_{i=1}^{N} |B(R_{mag}, L_{mag}, M_{mag})| = |B(\bar{x}, 0, 0)| < |B_{target}| \\ N = N_a \cdot N_{mag} \\ N_{mag} = \dfrac{2\pi R_s^2}{\pi R_{mag}^2} \\ N_a = \dfrac{\frac{2R_s\pi}{4} + R_{mag}}{2R_{mag}} \end{cases} \quad (15)$$

where $N$, $N_a$ e $N_{mag}$ are respectively the total number of magnets on the helmet, the number of rings and the number of magnets on each ring. The results of the optimization process led to the design of a helmet with 60 NdFeB magnets placed on the hemispherical support with radius $R_s$ = 12 cm, as shown in figure 3(b). Each magnet has a radius of $R_{mag}$ = 2 cm, a length of $L_{mag}$ = 30 cm and a magnetization $M_{mag} = 1.1{*}10^6\ \frac{A}{m}$ along its axis. A spherical symmetry arrangement was chosen for the magnets in order to optimize the magnetic field value at the center of the brain. Referring to a spherical coordinate system ($\rho$, $\phi$, $\theta$) (figure 4(a)), Neodymium magnets were arranged in a configuration of 5 rings at polar angular distance $\theta = 20°$. Angular position and number of magnets in each ring are shown in figure 4(b). This arrangement was chosen in order to optimize the number of magnets placed on the hemispherical support and therefore to generate the highest magnetic field value at the target site (in the worst case the tumor is located in the center of the brain).

## 4. Results

### 4.1. Magnetic field map

The map of the absolute value of the magnetic field generated by the helmet referring to the median plane of the head is shown in figure 5. The same magnetic field map can be evaluated in the sagittal plane because of the spherical symmetry arrangement of the magnets. As evident in figure 5, the magnetic field is smaller than $B_{target}$ (0.6 T) in most of the superficial regions of the brain. The helmet generates a magnetic field with values close to $B_{target}$ only at the central superficial area of the brain, where the maximum value for the magnetic field is $B_{max} = 0.580\ T$.

### 4.2. Capture efficacy maps

In order to evaluate the ability of the magnetic helmet to anchor the EMHVs at the target site, and therefore the therapeutic efficacy of the designed system in the glioma treatment, therapeutic efficacy maps were estimated. Such maps show the capture efficiency of the EMHVs at the tumor site, depending on the velocity of the blood and on the area where the glioma is located. The capture efficiency was defined as:

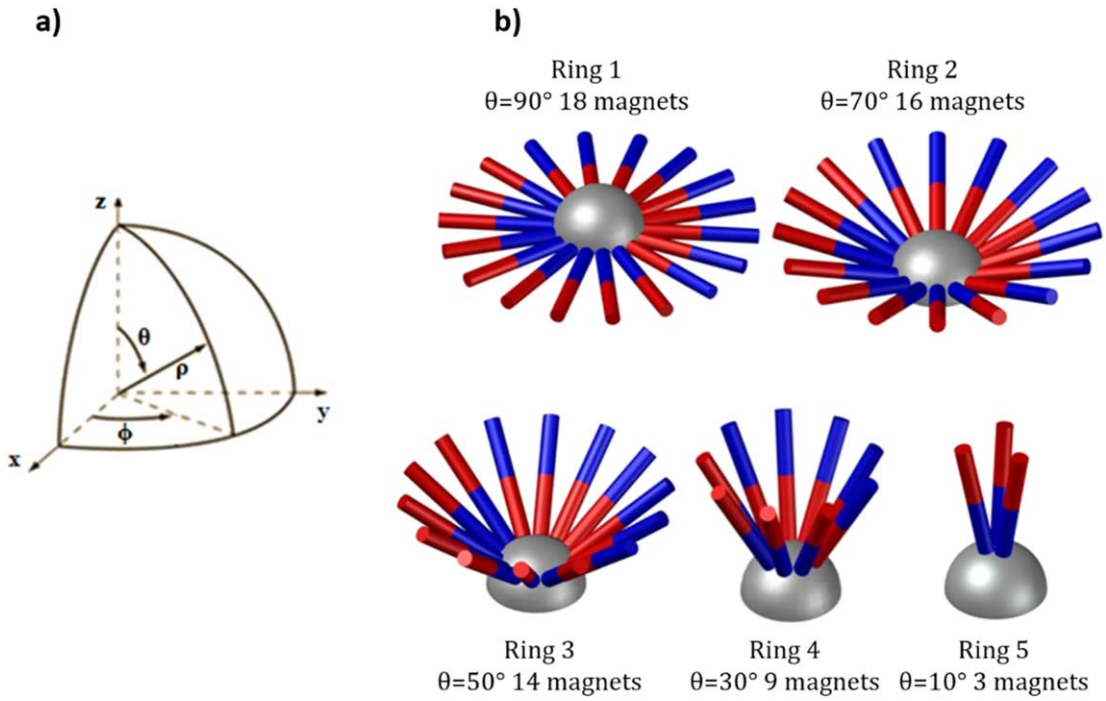


**Figure 4.** (a) Spherical coordinate system ($\rho, \phi, \theta$), (b) Different rings of magnets on the helmet: Ring 1 with 18 magnets, placed at polar angle $\theta = 90°$, Ring 2 with 16 magnets, placed at polar angle $\theta = 70°$, Ring 3 with 14 magnets, placed at polar angle $\theta = 50°$, Ring 4 with 9 magnets, placed at polar angle $\theta = 30°$,Ring 5 with 3 magnets, placed at polar angle $\theta = 1$.

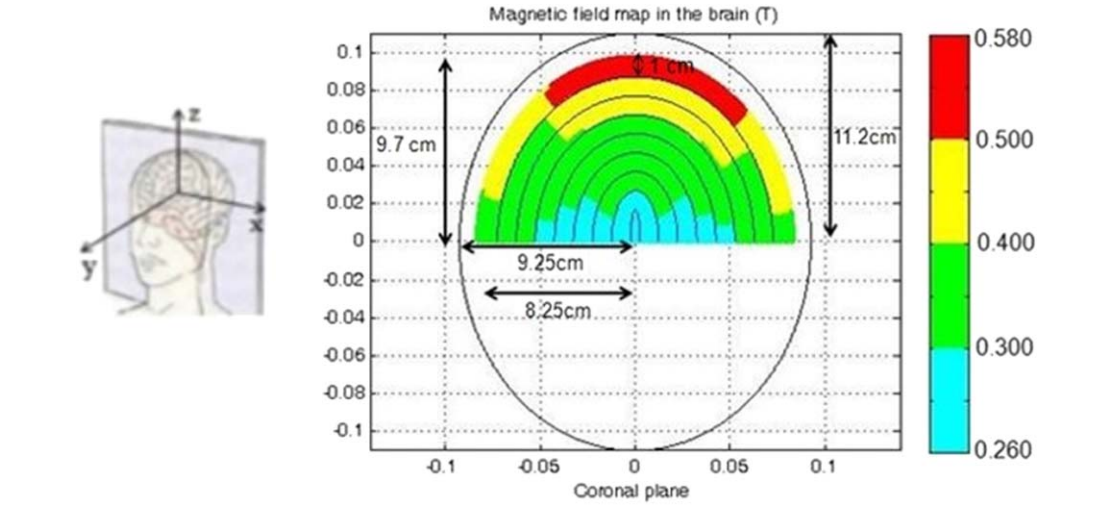


**Figure 5.** Magnetic field map generated by the magnetic helmet referring to the coronal plane of the human head.

$$\eta = \frac{N_{EMHVs,stop}}{N_{EMHVs,tot}} \tag{16}$$

where $N_{EMHVs,stop}$ and $N_{EMHVs,tot}$ are the number of EMHVs stopped in the target area thanks to the magnetic helmet and the total number of EMHVs inside the vessel, respectively.

The therapeutic efficacy maps were calculated for three values of the average blood flow velocity in the tumor arteriole taken to be in the range $0.1 \frac{\text{mm}}{\text{s}} \leqslant \bar{v}_f \leqslant 1 \frac{\text{mm}}{\text{s}}$ (these values represent the blood flow velocity in tumoral arterioles as reported in the literature (Rotariu and Strachan (2005)) (figures 6(a)–(c)). Considering the EMHVs moving in the tumor arteriole with the maximum average blood flow velocity $\bar{v}_f = 1 \frac{\text{mm}}{\text{s}}$, corresponding to the case study considered for the helmet design, the magnetic helmet allows to reach a capture efficiency $\eta = 75\%$ at the superficial and central region of the brain with a thickness of 1 cm. In particular, in such a region a maximum value of capture efficiency $\eta = 79\%$ was computed (figure 6(a)).

The efficacy of the magnetic helmet to target EMHVs tends to decrease with depth and reaches the lowest value $\eta = 58\%$ at the center of the brain

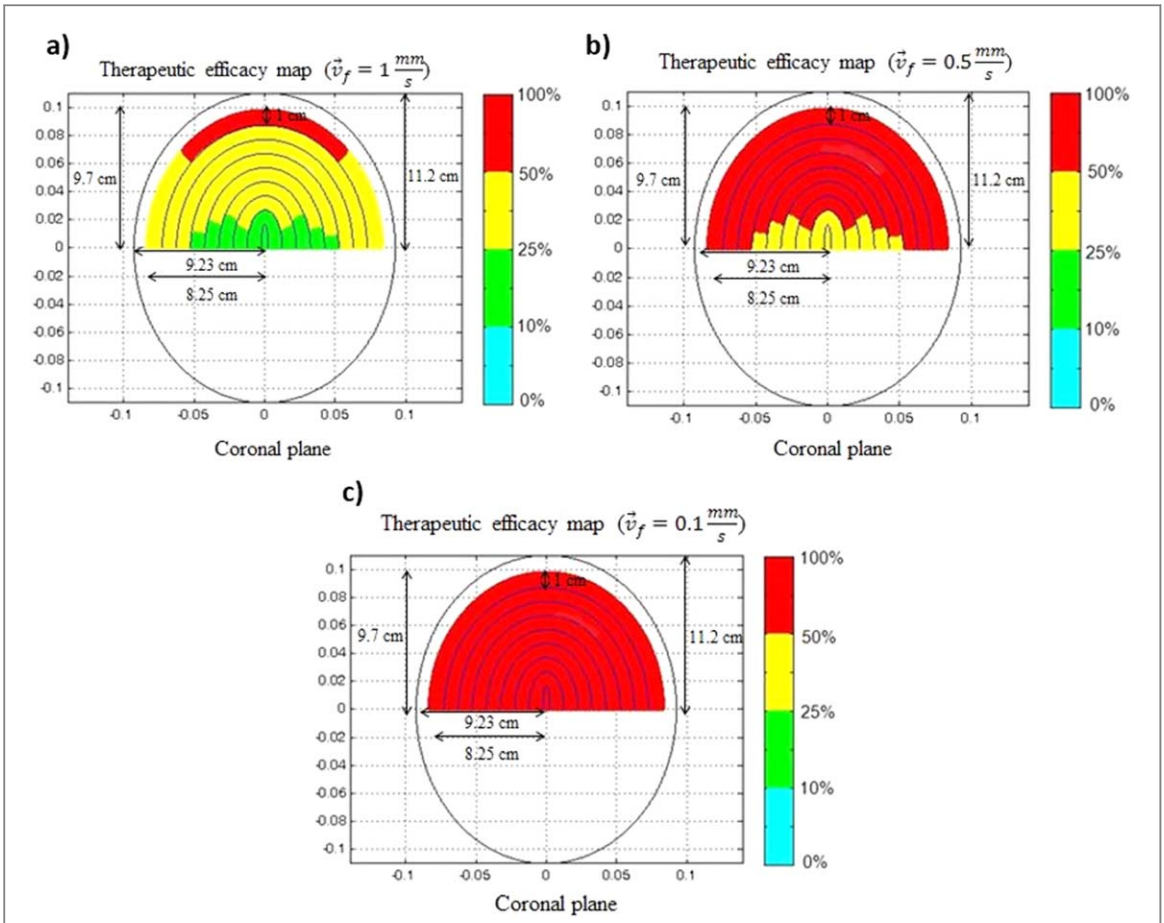


**Figure 6.** Therapeutic efficacy maps depending on the blood velocity, taking to be in the range 0.1 mm/s $\leqslant \bar{v}_f \leqslant$ 1 mm/s. In particular (a) $\bar{v}_f = 1$ mm/s (b) $\bar{v}_f = 0.5$ mm/s (c) $\bar{v}_f = 0.1$ mm/s.

(figure 6(a)). Decreasing the blood velocity in the tumor arteriole, the magnetic field necessary to anchor the EMHVs decreases and the capture efficacy of the magnetic helmet increases. In the case of EMHVs moving in the blood flow with velocity $\bar{v}_f = 0.5\ \frac{\text{mm}}{\text{s}}$, as shown in figure 6(b), a capture efficiency $\eta = 50\%$ is evaluated in the majority of the brain areas. A capture efficiency $\eta = 100\%$ was computed if the glioma is located at the superficial and central region of the brain and a minimum value $\eta = 36\%$ was observed at the center of the brain. The therapeutic efficacy map corresponding to the blood velocity $\bar{v}_f = 0.1\ \frac{\text{mm}}{\text{s}}$ (figure 6(c)) shows a capture efficiency of $\eta = 100\%$ all over the brain. Such value of capture efficiency was obtained because the magnetic field required to stop EMHVs moving with velocity $\bar{v}_f = 0.1\ \frac{\text{mm}}{\text{s}}$ is much less than the magnetic field generated by the magnetic helmet.

Interestingly, due to the difference in blood velocity between normal and tumor arterioles, by supposing the same spatial distribution of the regions (i.e., tumors and healthy) the capture efficiency in healthy regions is reduced of about a factor 10. In addition, in the case of glioma located at the center of the brain, EMHVs will not stop in healthy superficial regions, although in such regions there is a higher magnetic field value than that at the tumor site. As the blood velocity in the normal arterioles is greater than the blood velocity in tumor arterioles, the magnetic field required to anchor the EMHVs in healthy regions is much higher than that necessary to stop the EMHVs in the tumor sites.

In order to demonstrate it, an explicative example is reported below. We supposed a tumor as a sphere of radius r = 2.8 cm (i.e., it corresponds to ¼ of the radius of head) placed at the center of first quarter of the head (i.e., $\theta = 135°$ and a distance of the center of head of 5.6 cm) and a single vessel in its center with a blood velocity of 0.5 mm/s. as shown in figure 7.

The surrounding healthy regions are fed by four vessels symmetrically distributed around the tumor as reported in (a)–(d) points of figure 7 and the blood velocity was supposed to be 5 mm $s^{-1}$. In order to focus the magnetic field on the tumor the designed helmet was supposed to be rotated with an angle of 135° respect to figure 3(b). Considering that, the therapeutic efficacies in the tumor and healthy regions, respectively (i.e. in (a)–(c) and d points) were evaluated.

The results demonstrated a capture efficiency of $\eta_{tumor} = 89\%$ inside the tumor versus a capture efficiency of $\eta_{healthy} = 20.5\%$ in healthy regions

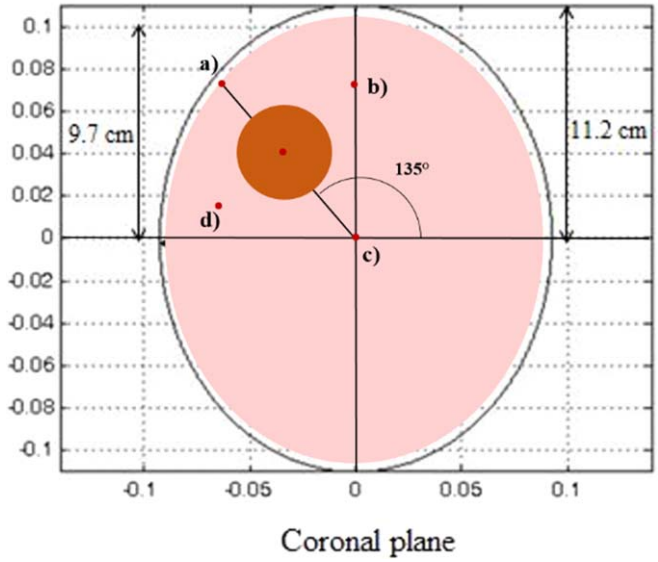


**Figure 7.** An example of different therapeutic efficiencies in tumor (brown) respect to the healthy (pink) regions. The therapeutic efficiency in tumor results to be $\eta_{\text{tumor}} = 89\%$ whereas in healthy results to be $\eta_{\text{healthy}} = 20.5\%$. The therapeutic efficiency in healthy regions was calculated as a mean value of the therapeutic efficiencies calculated in the points (a)–(d).

where $\eta_{healthy}$ is the mean values of $\eta_a = 37\%$, $\eta_b = \eta_d = 21\%$ and $\eta_c = 3.1\%$.

## 5. Discussion and conclusion

The objective of this paper was to design a wireless magnetic system for the treatment of brain cancers, able to anchor the EMHV DDS, moving in a tumor arteriole, at the target site.

The proposed idea was to design a system able to generate relevant magnetic field and magnetic force for human applications, in a compact form and inexpensively, differently from the magnetic actuation system (i.e., Octomag or MRI systems), proposed in the literature, which are cumbersome and with a restrictive workspace.

After computing the target value ($B_{target} = 0.6\ T$) required to anchor the EMHVs at the tumor site in the case of maximum velocity, i.e., supposed to be at the center of the brain, by an analytical model several magnetic and fluid dynamic simulations and parametric studies were carried out in order to obtain the optimal configuration (see section 3.4) in terms of sizes, number and magnetization of the NdFeB magnets. The spherical symmetry arrangement of the NdFeB magnets on the hemispherical support was chosen to optimize the magnetic field value in the deeper region of the brain. Although the system is not able to generate magnetic fields close to the magnetic field $B_{target}$ at the center of the brain, taking into account the geometric constraints due to the size of the patient's head and the need to limit the helmet dimensions, the configuration of the NdFeB magnets used in the study is the optimal solution in order to generate high magnetic fields at big distances. Moreover, the proposed magnetic system is a versatile system that allows for varying the number and the inclination of the NdFeB magnets depending on the tumor site. In the case of gliomas located at the surface of the brain, only the NdFeB magnets located on the hemispherical support above the tumor site could be used during the tumor treatments. By varying the inclination of the magnets depending on the tumor position, it is possible to optimize the magnetic field value in the region where the tumor is located.

The magnetic helmet was designed for the capture of EMHVs moving in the tumor arteriole having the maximum blood flow velocity. By evaluating the capture efficiency of the EMHVs DDS and the efficacy of the magnetic system varying the blood velocity in the tumor arterioles, it was noticed that the magnetic helmet shows relevant values of capture efficiency in deep regions of the brain if the EMHVs move in the arteriole with blood flow velocity $\bar{v}_f \leqslant 0.5\ \frac{\text{mm}}{\text{s}}$. In this case the proposed magnetic helmet could be used for the treatment of deep gliomas by using EMHV DDS. Considering the EMHVs moving with the maximum blood velocity $\bar{v}_f = 1\ \frac{\text{mm}}{\text{s}}$, the magnetic helmet is more effective for the treatment of superficial tumors.

It is worth mentioning that, although the mechanism of pharmacological release by the EMHVs occurs at a capillary level, the approximation of the EMHV moving in the arteriole is acceptable, giving the possibility to study the EMHV's behavior under the effect of a realistic drag force with reduction of the computational cost of simulations. In fact, in this study, arteriolar blood was considered as a Newtonian fluid without turbulence, but higher blood flow

velocities in the arteriole were used with respect to the capillary.

In conclusion, the magnetic helmet designed in the study is an innovative model of a magnetic generation system to be used for the location of drug-carrying magnetic agents like EMHVs and the treatment of human brain cancer. Although the platform was proposed for the treatment of cerebral tumors in this study, its use could be extended for the treatment of additional pathologies where a localized pharmacological approach is required, such as Alzheimer's and Parkinson's diseases (Karthivashan *et al* (2018), Agrawal *et al* (2020), Nirale *et al* (2020)).

Future studies will focus on the development of the proposed magnetic helmet and its experimental validation *in vitro* and *in vivo*.

## ORCID iDs

Gioia Lucarini https://orcid.org/0000-0003-2725-6658

## References

Abbott N J 2013 Blood-brain barrier structure and function and the challenges for CNS drug delivery *Journal of Iherited Metabolic Disease* **36** 437–49

Agrawal M, Saraf S, Saraf S, Dubey S K, Puri A, Patel R J and Alexander A 2020 Recent strategies and advances in the fabrication of nano lipid carriers and their application towards brain targeting *J. Controlled Release* **321** 372–415

Batchelor G K 2000 *An Introduction in Fluid Dynamics* (Cambridge, UK: Cambridge University Press)

Bushby K M D, Cole T, Matthews J N S and Goodship J A 1992 Centiles for adult head circumference *Archives of Disease in Childhood* **67** 1286–7

Cinti C, Taranta M, Naldi I and Grimaldi S 2011 Newly engineered magnetic erythrocytes for sustained and targeted delivery of anti-cancer therapeuticcompounds *PLoS One* **6** e17132

Furlani E P and Ng K C 2006 Analytical model of magnetic nanoparticle transport and capture in the microvasculature *Phys. Rev.* E **73** 061919

Greish K 2010 Enhanced permeability and retention (EPR) effect for anticancer nanomedicine drug targeting *Cancer Nanotechnology: Methods and Protocols* **624** 25–37

Grifantini R *et al* 2018 Magnetically driven drug delivery systems improving targeted immunotherapy for colon-rectal cancer *J. Controlled Release* **280** 76–86

Haverkort J V, Kenjeres S and Kleijin C R 2009 Magnetic particle motion in a Poiseuille flow *Phys. Rev.* **E80** 016302

Jones T P 1995 *Electromechanics of Particles* (Cambridge, UK: Cambridge University Press)

Karthivashan G, Ganesan P, Park S Y, Kim J S and Choi D K 2018 Therapeutic strategies and nano-drug delivery applications in management of ageing Alzheimer's disease *Drug Delivery* **25** 307–20

Lande C *et al* 2012a Engineered magnetic erythrocyte applied for local gene therapy to prevent restenosis CARDIOVASCULAR RESEARCH, SUPPLEMENT

Lande C *et al* 2012b P416engineered magnetic erythrocyte applied for local gene therapy to prevent restenosis *Cardiovascular Res.* **93** .suppl_1 S52–87

Lande C *et al* 2012c Innovative erythrocyte-based carriers for gene delivery in porcine vascular smooth muscle cells: basis for local therapy to prevent restenosis *Cardiovascular & Haematological Disorders-Drug Targets (Formerly Current Drug Targets-Cardiovascular & Hematological Disorders)* **12** 68–75

Lande C *et al* 2012 Innovative Erytro-Magneto-HA Virosomes for gene-drug delivery in porcine model of VSMC activation: basis for local therapy to prevent restenosis *Cardiovasular & Hematological Disorders. Drug Targets* **12** 68–75

Liu J F *et al* 2019 Use of magnetic fields and nanoparticles to trigger drug release and improve tumor targeting *Wiley Interdiscip. Rev. Nanomed. Nanobiotechnol.* **11** e1571

Lunnoo T and Puangmali T 2015 Capture efficiency of biocompatible magnetic nanoparticles in arterial flow: a computer simulation for magnetic drug targeting *Nanoscale Res. Lett.* **10** 426

Moghimi S M, Hunter A C and Murray J C 2001 Long-circulating and target-specific nanoparticles: thery to practice *Pharmacolical Reviews* **53** 283–318

Mura S, Nicolas J and Couvreur P 2013 Stimuli-responsive nanocarriers for drug delivery *Nat. Mater.* **12** 991–1003

Muzykantov V R 2010 Drug delivery by red blood cells: vascular carriers designed by Mother Nature *Expert Opin Drug Deliv.* **7** 403–27

Naldi I *et al* 2014 Novel epigenetic target therapy for prostate cancer: a preclinical study *PLoS One* **9** e98101

Nirale P, Paul A and Yadav K S 2020 Nanoemulsions for targeting the neurodegenerative diseases: Alzheimer's, Parkinson's and Prion's *Life Sci.* **245** 117394

Ostrom Q T, Gittleman H, Farah P, Ondracek A, Chen Y, Wolinsky Y, Stroup N E, Kruchko C and Barnholtz-Sloan J S 2013 CBTRUS statistical report: primary brain and central nervous system tumors diagnosed in the United States in 2006–2010 *Neuro-Oncology* **15** 1–56

Pierige F, Serafini S, Rossi L and Magnani M 2008 Cell-based drug delivery *Adv. Drug Delivery Rev.* **60** 286–95

Poston A 2000 Static adult human physical characteristics of the adult head *Department of Defense Human Factors Engineering Technical Advisory Group (DOD-HDBK-743A)* **75** 72–5

Price P M *et al* 2018 Magnetic drug delivery: Where the field is going *Frontiers in Chemistry* **6** 619

Ricotti L, Cafarelli A, Iacovacci V, Vannozzi L and Menciassi A 2015 Advanced micro-nano-bio systems for future targeted therapies *Current Nanoscience* **11** 144–60

Rossi L, Serafini S, Pierigé F, Antonelli A, Cerasi A, Fraternale A and Magnani M 2005 Erythrocyte-based drug delivery *Expert Opinion on Drug Delivery* **2** 311–22

Rotariu O and Strachan N J C 2005 Modelling magnetic carrier particle targeting in the tumor microvasculature for cancer treatment *J. Magn. Magn. Mater.* **293** 639–46

Tabatabaei S N *et al* 2015 Remote control of the permeability of the blood–brain barrier by magnetic heating of nanoparticles: a proof of concept for brain drug delivery *J. Controlled Release* **206** 49–57

Timko B P, Dvir T and Kohane D S 2010 Remotely triggerable drug delivery systems *Adv. Mater.* **22** 4925–43

Vennemann P, Lindken R and Westerweel J 2007 *In vivo* whole-field blood velocity measurement techniques *Exp. Fluids* **42** 495–511

Wilhelm S *et al* 2016 Analysis of nanoparticle delivery to tumours *Nature Reviews Materials* **1** 16014